Priority Report

Cancer Research

A Cancer Detection Platform Which Measures Telomerase Activity from Live Circulating Tumor Cells Captured on a Microfilter

Tong Xu[1], Bo Lu[2], Yu-Chong Tai[2], and Amir Goldkorn[1]

Abstract

Circulating tumor cells (CTC) quantified in cancer patients' blood can predict disease outcome and response to therapy. However, the CTC analysis platforms commonly used cannot capture live CTCs and only apply to tumors of epithelial origin. To address these limitations, we have developed a novel cancer detection platform which measures telomerase activity from live CTCs captured on a parylene-C slot microfilter. Using a constant low-pressure delivery system, the new microfilter platform was capable of cell capture from 1 mL of whole blood in less than 5 minutes, achieving 90% capture efficiency, 90% cell viability, and 200-fold sample enrichment. Importantly, the captured cells retained normal morphology by scanning electron microscopy and could be readily manipulated, further analyzed, or expanded on- or off-filter. Telomerase activity—a well-recognized universal cancer marker—was reliably detected by quantitative PCR from as few as 25 cancer cells added into 7.5 mL of whole blood and captured on the microfilter. Moreover, significant telomerase activity elevation was also measured from patients' blood samples and from single cancer cells lifted off of the microfilter. Live CTC capture and analysis is fast and simple yet highly quantitative, versatile, and applicable to nearly all solid tumor types, making this a highly promising new strategy for cancer detection and characterization. *Cancer Res; 70(16); 6420–6. ©2010 AACR.*

Introduction

Circulating tumor cells (CTC) captured from peripheral blood were recently shown to predict disease outcome and therapy response in cancer patients (1–7). Currently, CTCs are isolated from blood by methods which rely on immunomagnetic binding of cell surface epithelial cell adhesion molecules (EpCAM), an expensive, labor-intensive approach that is limited to EpCAM-expressing tumors (7, 8). We previously reported an alternative platform using a novel parylene-C pore microfilter which traps CTCs quickly and efficiently based on their size differential from other blood cells (9). However, like the EpCAM-based approach, our pore microfilter relied on fixation, staining, and visual enumeration of captured cells, a laborious and subjective process prone to reader/operator variability. These limitations can be surmounted by measuring telomerase activity from microfilter-captured live CTCs. As a CTC biomarker, telomerase activity offers several advantages: (*a*) it is a widely applicable tumor marker with validated diagnostic and prognostic utility in multiple cancer types (10–17); (*b*) it is a uniquely "functional" assay that reflects the presence of live cancer cells; (*c*) it can be amplified and measured accurately from small numbers of cells using quantitative PCR (qPCR) without the need to visualize or count the cells; and (*d*) it can be scaled-up cheaply and rapidly to yield quantitative, operator-independent results. Reasoning that such an approach would be widely applicable to nearly all solid tumor types regardless of EpCAM expression, we set out to develop a novel microfilter-based platform capable of measuring telomerase activity from live-captured CTCs.

Materials and Methods

Filter fabrication

A 10-μm-thick parylene-C layer was deposited on prime silicon wafer (Fig. 1A). Then, either Cr/Au or Al was deposited using a thermal evaporator, followed by wet-etch patterning. Using the metal layer as a mask, an array of 30,401 slot openings was etched through the parylene-C membrane by reactive ion etching. Lastly, the parylene-C membrane was peeled off from the silicon substrate.

Constant pressure fluid delivery system

Pressure from a nitrogen tank was reduced to <1 psi by a two-stage regulator (Fig. 1C) and further downregulated

Authors' Affiliations: [1]Division of Medical Oncology, Department of Internal Medicine, Norris Comprehensive Cancer Center, Keck School of Medicine, University of Southern California, Los Angeles, California and [2]Electrical Engineering, California Institute of Technology, Pasadena, California

Note: Supplementary data for this article are available at Cancer Research Online (http://cancerres.aacrjournals.org/).

T. Xu and B. Lu contributed equally to this work.

Corresponding Author: Amir Goldkorn, 1441 Eastlake Avenue, Suite 3440, Los Angeles, CA 90033. Phone: 323-442-7721; Fax: 323-865-0061; E-mail: agoldkor@usc.edu.

doi: 10.1158/0008-5472.CAN-10-0686

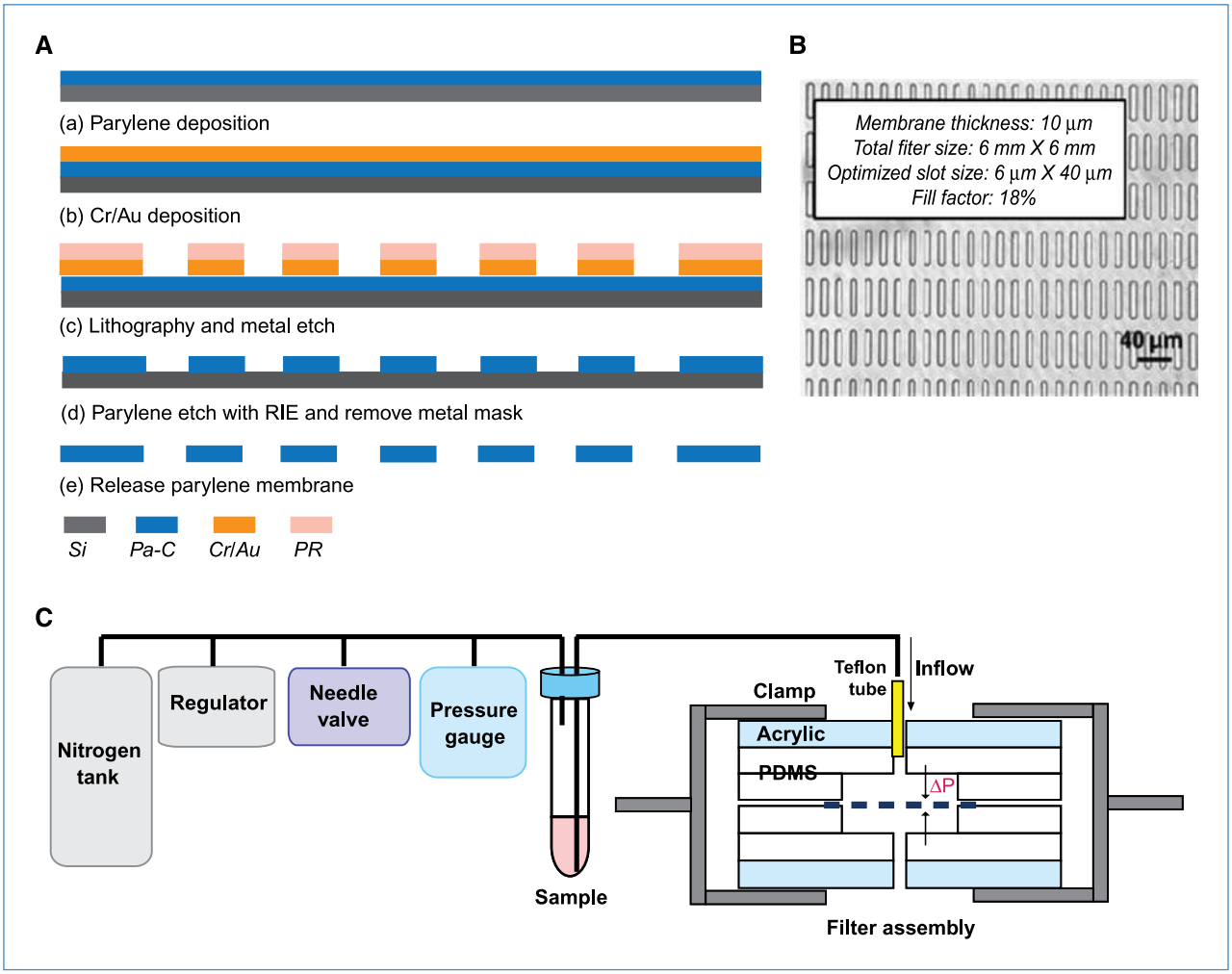

Figure 1. Microfilter fabrication and constant-pressure fluid delivery system. A, microfilter fabrication process. B, bright-field micrograph of slot microfilter. C, constant-pressure fluid delivery system and filter assembly.

accurately by adjusting a needle valve to 0.1 to 0.13 psi. A 15 mL conical tube containing the sample was connected as a reservoir. The filter was sandwiched between two thin pieces of polydimethylsiloxane with wells and then clamped between polydimethylsiloxane/acrylic jigs to form a sealed chamber.

Cell lines

PC3 and DU145 human prostate cancer cell lines were generously provided in 2007 by the laboratory of Elizabeth Blackburn (University of California San Francisco) and were not re-authenticated prior to use in these experiments. Both cell lines were maintained in standard culture conditions (RPMI/10% fetal bovine serum at 37°C).

Capture efficiency, cell viability, and enrichment

PC3 and DU145 cancer cells were stained with Calcein-AM fluorescent dye, and 10 cells were added to 1 mL of human blood. After filtration, captured cells were costained with propidium iodide on filter and counted under a fluorescent microscope (Z1 microscope, Zeiss Imager) with Axiovision software. Viable Calcein-AM–retaining cells were fluorescent green whereas dead cells were fluorescent red following propidium iodide staining.

Capture efficiency was calculated as

$$\text{Capture efficiency}\ (\%) = \frac{\text{cancer cells (green + red) on filter}}{\text{cancer cells added to blood}} \times 100.$$

Cell viability was calculated as

$$\text{Cell viability}\ (\%) = \frac{\text{green fluorescent cells}}{\text{total captured cancer cells (green + red)}} \times 100.$$

Enrichment was determined by staining and counting the peripheral blood mononuclear cells (PBMC) remaining on the filter with acridine orange and was calculated as

$$\text{Enrichment(fold)} = \frac{(\text{cancer cells/PBMCs})_{\text{on filter postfiltration}}}{(\text{cancer cells/PBMCs})_{\text{original blood sample}}}$$

Standard volume blood samples (7.5 mL) were processed similarly but with the addition of Ficoll-Paque gradient centrifugation and resuspension in 2 mL of PBS.

Patient specimen collection and processing

Blood samples (7.5 mL) were drawn from patients with metastatic prostate cancer under an Institutional Review Board–approved protocol, as well as from healthy volunteer controls into EDTA K2 vacutainer tubes, and processed within 24 hours.

Scanning electron microscopy

The microfilter containing captured cells was processed according to standard protocols, and then photographed on a scanning electron microscope at ×3,500 magnification (JEOL JSM/6390LV).

Telomeric repeat amplification protocol assay

Telomerase activity from cell extracts was analyzed using a previously described real-time PCR–based telomeric repeat amplification protocol (TRAP; ref. 18).

Statistics

All cell capture and telomerase activity experiments were performed in triplicate and reported with SE bars. Telomerase activity (Ct) mean and specificity range for true negatives (healthy cohort) were calculated using the SAS statistical package, version 9.2. Telomerase activity (Ct) differences for filtration in series between filters 1, 2, and 3 were compared using ANOVA. All tests were two-sided at a 0.05 significance level, and were performed using the SAS statistical package, version 9.2.

Results

We used parylene-C because of its mechanical strength and flexibility, biocompatibility, and easy machinability. The microfilter was fabricated by a multistep deposition and etching process (Fig. 1A; Materials and Methods), resulting in an array of 30,401 slot openings. We chose a slot design to maximize cellular deformation and passage of blood cells in the longitudinal axis while capturing the larger and less deformable CTCs (Fig. 1B). The slot design generated a large fill factor (~18%), thus greatly reducing the flow resistance and pressure gradient (ΔP) across the filter, critical for preserving the structural integrity and viability of live CTCs. To achieve reproducible and gentle delivery of unfixed samples, we assembled a constant low-pressure system consisting of a nitrogen pressure source in series with a pressure regulator and fine-pressure valves capable of driving the sample with an accuracy of ±0.01 psi (Fig. 1C).

To optimize the microfilter slot width and drive pressure, we tested various designs using whole blood samples (1 mL) and added 10 PC3 prostate cancer cells. All tested slot widths were considerably smaller than the mean PC3 cancer cell diameter, resulting in similar capture efficiencies of ~90% (Fig. 2A). However, cellular viability was significantly diminished from 90% to 70% at the larger (7 μm) slot width, possibly because the cells became more deeply "wedged" into the wider slots and sustained greater deformation and mechanical damage. On the other hand, CTC enrichment diminished from 200-fold to only 70-fold at the smaller slot width (5 μm), because many more PBMCs were trapped along with the CTCs. Therefore, we settled on an optimal slot width of 6 μm, which provided the highest capture efficiency (90%), cell viability (90%), and enrichment (200-fold) of cancer cells relative to PBMCs.

The 6 μm slot filter was used to determine the optimal filtration drive pressure, and ultimately, 0.13 psi was chosen as the optimal pressure for speed, capture efficiency, and viability (Fig. 2A). This pressure preserved the morphology of captured cells (Fig. 2B) and allowed the filtration of 1 mL of whole blood in less than 5 minutes, a capture rate that is ~10-fold faster than that of other recently published microfluidic platforms (8).

We validated these slot and pressure parameters for capture of cells from a standard 7.5 mL blood sample. After Ficoll-Paque gradient centrifugation (to reduce sample volume and eliminate RBC), the optimized filtration settings yielded ~70% capture efficiency, 90% viability, and 1,500-fold enrichment (Fig. 2C). The viability of captured cancer cells was further validated by expanding the cells in culture either directly on filter or by first washing them into a culture dish (Fig. 2D). Notably, the microfilter provided a biocompatible environment for cancer cell adherence and growth.

We tested whether telomerase activity could be detected from live-captured cancer cells by spiking DU145 prostate cancer cells into 7.5 mL of whole blood, then lysing the live-captured cells on the filter and analyzing the lysate by qPCR-TRAP (Fig. 3A). Remarkably, this method was capable of detecting as few as 25 cancer cells added to 7.5 mL of whole blood (Fig. 3A, $P = 0.01$ for each spiked sample compared with blood only), and the threshold cycle value (Ct) value was inversely proportional and linearly correlated with the number of spiked cells (Fig. 3B). To test whether cell capture and the telomerase signal degraded significantly over 24 hours, we added 100 cancer cells into 1 mL aliquots of whole blood drawn from three healthy donors and kept the samples at room temperature for 1, 6, 12, and 24 hours prior to processing. At all time points, the assay yielded statistically significant positive telomerase activity readings; activity was essentially unchanged in the first 6 hours, and there was a subsequent trend (not statistically significant) towards lower activity at 12 and 24 hours (Supplementary Fig. S1).

We conducted a limited proof-of-principle experiment wherein blood samples from 15 healthy donors and 13 cancer patients were tested (Fig. 3C) using slot microfilter capture and qPCR-TRAP. Among healthy donors, the average Ct was 33.9 ± 1.32. To maximize assay specificity based on this true negative cohort, we defined Ct = 33 as the cut-off threshold for a positive telomerase activity assay, thus yielding a specificity of 93% (95% confidence interval, 68–100%) within the training set of healthy donors. When a

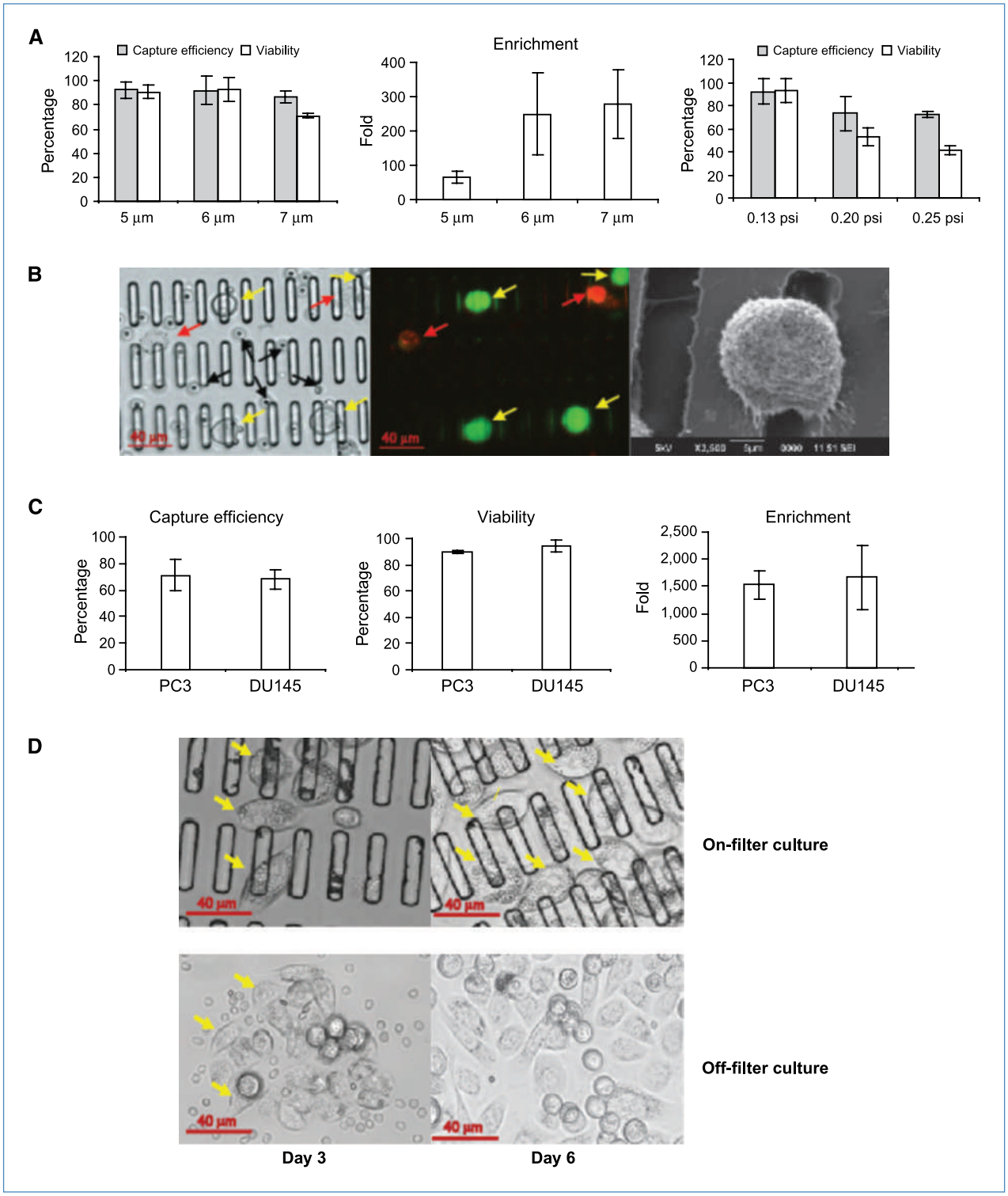

Figure 2. Microfilter optimization and validation. A, slot size and filtration pressure optimization. Left, comparison of cell capture efficiency and viability with different slot sizes. Center, measurement of enrichment with different slot sizes. Right, comparison of capture efficiency and viability with various filtration pressures using a 6-µm slot filter. B, cancer cells captured on microfilter and imaged under bright-field (left) and fluorescence (center) of the same field; yellow arrows, live captured cancer cells; red arrows, dead cancer cells; black arrows, PBMCs. Right, scanning electron microscopy of captured cancer cell. C, validation of cancer cell capture from 7.5 mL whole blood. Shown are capture efficiency (left), cell viability (middle), and enrichment (right). D, on-filter (top) and off-filter (bottom) cell culture of PC3 cells captured from whole blood after 3 and 6 d. Yellow arrows denote foci of cancer cell proliferation. All histogram results are means of triplicate independent experiments.

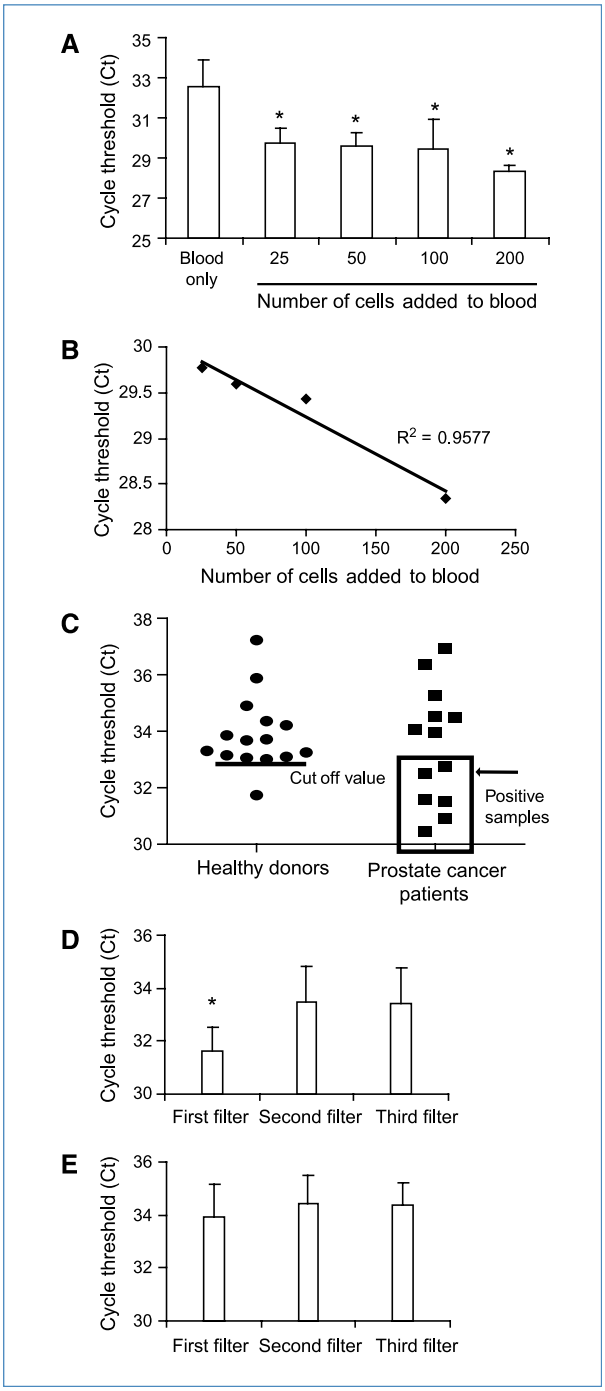

Figure 3. Detection of telomerase activity from live cancer cells captured on a slot microfilter. A, telomerase activity detected from 7.5 mL blood samples spiked with a range of cancer cell numbers or blood only (P = 0.01 for each sample compared with blood-only sample). B, linear correlation of Ct values with the number of cells added. All histogram results are means of triplicate independent experiments. C, telomerase activity of patient samples versus healthy donor controls. The line in healthy donors indicates the calculated true negative Ct cutoff value of 33; patient samples falling within the positive range (Ct < cutoff value) are boxed. D, serial filtration to internally control for PBMC background telomerase activity on six positive patient samples (P = 0.029). E, serial filtration on healthy donor samples (P = 0.5).

test cohort of patient samples was tested using this cutoff, 6 of 13 patients were found to have Ct values below the threshold of Ct = 33. These six patients with positive CTC telomerase activity assays had a mean Ct of 31, ~8-fold telomerase activity relative to the mean telomerase activity of the healthy control cohort.

We internally controlled the telomerase activity assay for intersample variability such as fluctuations in background PBMC by passing each sample through three microfilters in series. When this approach was applied to the six telomerase-positive cancer patients identified above, telomerase activity was significantly higher in the first filter (reflecting captured CTCs) than in the second or third filters (reflecting background PBMCs; Fig. 3D; ANOVA, P = 0.029). In contrast, there was no significant telomerase activity difference between the first, second, and third filters in the other seven patients with low telomerase activity (ANOVA, P = 0.28; data not shown), or between serial filters in healthy donors (Fig. 3E; ANOVA, P = 0.51). This approach further strengthened the assay by enabling telomerase activity readings to be internally controlled for PBMC background and intersample variability.

We tested whether the platform would support single-cell analysis of live-captured cells. PC3 cancer cells were captured from whole blood on microfilter, localized by immunofluorescent staining (PE-conjugated anti-CD49 antibody), and recovered individually using a micropipette mounted onto a XYZ manipulating stage (Fig. 4). Single cancer cells were deposited in CHAPS lysis buffer and subjected to qPCR-TRAP, which yielded a significantly elevated telomerase activity level relative to negative controls.

Discussion

Here, we present a novel cancer biomarker platform capable of assaying telomerase activity in live CTCs captured from human blood. This new platform offers several important advances: most current cell capture techniques which rely on immune enrichment are limited to tumor types that express the cell surface antigen being targeted (usually EpCAM; refs. 7, 8); however, EpCAM expression can be quite variable (19) or even downregulated (20) in disseminating epithelial tumor cells. Furthermore, existing systems either require prior sample fixation and do not yield live CTCs, or capture live cells in a manner that is slow and precludes the removal of cells for further study (7–9). In contrast, the new slot microfilter is capable of rapidly and efficiently capturing live CTCs that can be studied on- or off-filter, enabling sophisticated characterization, and possibly, the expansion of these cells for further study.

The current slot microfilter design achieves viable cell capture without fixation and yields statistically significant telomerase activity up to 24 hours from the time of blood draw, with a moderate (nonsignificant) drop-off in activity from 12 to 24 hours, an ample time window for on-site, same-day processing of blood samples. Future microfilter platforms could be envisioned to integrate a compact

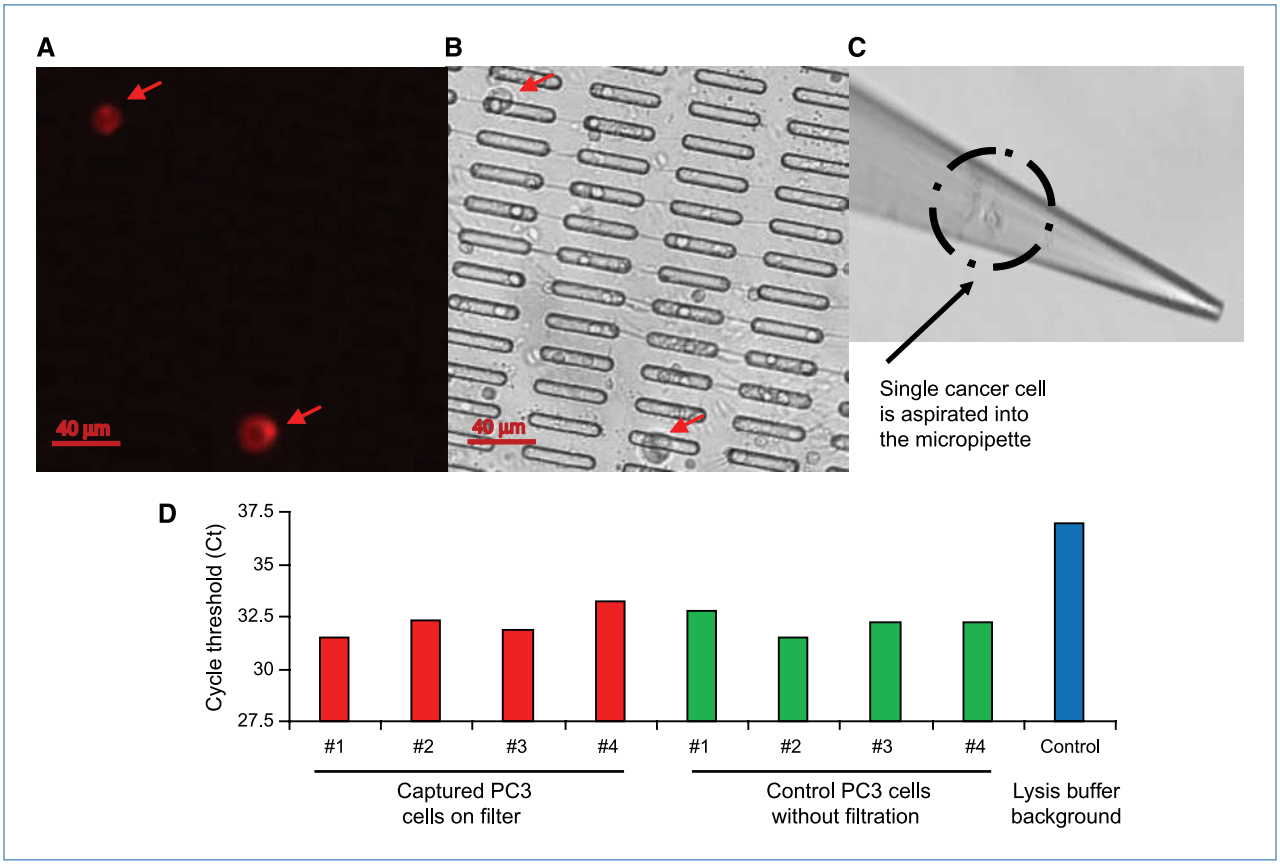

Figure 4. Telomerase activity measurement from single live cancer cells captured on a microfilter. A, captured cells stained by PE-CD49b. B, matched bright-field image. C, micropipette recovery of a single cell. D, single cell telomerase activity assays.

constant pressure delivery cartridge with the filter chamber to produce a simple point-of-care device for the processing of blood samples. The current platform design also uses Ficoll-Paque centrifugation for 7.5 mL blood samples; predictably, this additional step causes some loss (~20%) of capture efficiency; nevertheless, a 70% capture rate from 7.5 mL of whole blood in 15 minutes still compares quite favorably with other technologies (7–9). Future platforms will eliminate the Ficoll step for large volume processing via use of hydrophobically coated filters for reduced resistance, as well as multiple filters for parallel processing of smaller volumes.

Measurement of telomerase activity from live CTCs on slot microfilter constitutes a tumor biomarker strategy with broad applicability. Telomerase activity is a well-recognized cancer marker in >90% of human malignancies (15) and therefore is ideally suited to the microfilter, which can capture CTCs across all tumor types regardless of surface markers. Telomerase activity also constitutes a uniquely "functional" assay which reflects the presence of live cancer cells. Moreover, qPCR-TRAP can amplify the telomerase activity signal from as few as one cancer cell, raising the prospect of applying CTC-telomerase for early detection of occult malignancy.

The current platform is capable of detecting telomerase activity from as few as 25 cancer cells seeded into 7.5 mL of whole blood. It might be possible to increase platform sensitivity by further reducing the capture of background PBMCs (e.g., hydrophobically coated filters). On the other hand, the current detection level may already be sufficient to identify clinically significant disease, because the absolute range of significant CTC numbers has not been defined to date (each platform is biased by its own capture strategy). Another factor which might affect telomerase activity measurement is potential PBMC variability in various clinical states such as inflammatory conditions (increased PBMC telomerase) or chemotherapy (decreased PBMC numbers). This variability is addressed to a large extent by processing each blood sample through three filters in series and recording the difference in telomerase activity between the first filter (where CTCs are caught) and the second and third filters (which contain background PBMCs), thus internally controlling each assay for its individual blood sample.

Low-pressure slot microfiltration offers new and versatile capabilities for live CTC capture and analysis. The detection of telomerase activity highlights the potential utility of this novel platform, which can be applied to advance cancer research and enhance patient care.

Disclosure of Potential Conflicts of Interest

The authors' institutions (Cal Tech and USC) have submitted patent applications (pending) based on the new technologies presented in this manuscript.

Acknowledgments

The authors thank Dr. David I. Quinn for his critical review of this manuscript and his ongoing support of these studies.

Grant Support

Funded in part by NCI K08 CA126983-01 (AG).

The costs of publication of this article were defrayed in part by the payment of page charges. This article must therefore be hereby marked *advertisement* in accordance with 18 U.S.C. Section 1734 solely to indicate this fact.

Received 02/25/2010; revised 05/26/2010; accepted 06/21/2010; published OnlineFirst 07/27/2010.

References

1. Cohen SJ, Punt CJ, Iannotti N, et al. Relationship of circulating tumor cells to tumor response, progression-free survival, and overall survival in patients with metastatic colorectal cancer. J Clin Oncol 2008;26:3213–21.
2. de Bono JS, Scher HI, Montgomery RB, et al. Circulating tumor cells predict survival benefit from treatment in metastatic castration-resistant prostate cancer. Clin Cancer Res 2008;14:6302–9.
3. Gasent Blesa JM, Alberola Candel V, Esteban Gonzalez E, et al. Circulating tumor cells in breast cancer: methodology and clinical repercussions. Clin Transl Oncol 2008;10:399–406.
4. Goodman OB, Jr., Fink LM, Symanowski JT, et al. Circulating tumor cells in patients with castration-resistant prostate cancer baseline values and correlation with prognostic factors. Cancer Epidemiol Biomarkers Prev 2009;18:1904–13.
5. Ignatiadis M, Xenidis N, Perraki M, et al. Different prognostic value of cytokeratin-19 mRNA positive circulating tumor cells according to estrogen receptor and HER2 status in early-stage breast cancer. J Clin Oncol 2007;25:5194–202.
6. Shaffer DR, Leversha MA, Danila DC, et al. Circulating tumor cell analysis in patients with progressive castration-resistant prostate cancer. Clin Cancer Res 2007;13:2023–9.
7. Cristofanilli M, Budd GT, Ellis MJ, et al. Circulating tumor cells, disease progression, and survival in metastatic breast cancer. N Engl J Med 2004;351:781–91.
8. Nagrath S, Sequist LV, Maheswaran S, et al. Isolation of rare circulating tumour cells in cancer patients by microchip technology. Nature 2007;450:1235–9.
9. Zheng S, Lin H, Liu JQ, et al. Membrane microfilter device for selective capture, electrolysis and genomic analysis of human circulating tumor cells. J Chromatogr A 2007;1162:154–61.
10. Bravaccini S, Sanchini MA, Amadori A, et al. Potential of telomerase expression and activity in cervical specimens as a diagnostic tool. J Clin Pathol 2005;58:911–4.
11. Hiyama E, Saeki T, Hiyama K, et al. Telomerase activity as a marker of breast carcinoma in fine-needle aspirated samples. Cancer 2000;90:235–8.
12. Marchetti A, Bertacca G, Buttitta F, et al. Telomerase activity as a prognostic indicator in stage I non-small cell lung cancer. Clin Cancer Res 1999;5:2077–81.
13. Meeker AK. Telomeres and telomerase in prostatic intraepithelial neoplasia and prostate cancer biology. Urol Oncol 2006;24:122–30.
14. Poremba C, Willenbring H, Hero B, et al. Telomerase activity distinguishes between neuroblastomas with good and poor prognosis. Ann Oncol 1999;10:715–21.
15. Shay JW, Bacchetti S. A survey of telomerase activity in human cancer. Eur J Cancer 1997;33:787–91.
16. Streutker CJ, Thorner P, Fabricius N, Weitzman S, Zielenska M. Telomerase activity as a prognostic factor in neuroblastomas. Pediatr Dev Pathol 2001;4:62–7.
17. Wright WE, Piatyszek MA, Rainey WE, Byrd W, Shay JW. Telomerase activity in human germline and embryonic tissues and cells. Dev Genet 1996;18:173–9.
18. Xu T, Xu Y, Liao CP, Lau R, Goldkorn A. Reprogramming murine telomerase rapidly inhibits the growth of mouse cancer cells *in vitro* and *in vivo*. Mol Cancer Ther 2010;9:438–49.
19. Went PT, Lugli A, Meier S, et al. Frequent EpCam protein expression in human carcinomas. Hum Pathol 2004;35:122–8.
20. Polyak K, Weinberg RA. Transitions between epithelial and mesenchymal states: acquisition of malignant and stem cell traits. Nat Rev Cancer 2009;9:265–73.